Magnetic field mapping around metal implants using an asymmetric spin-echo MRI sequence

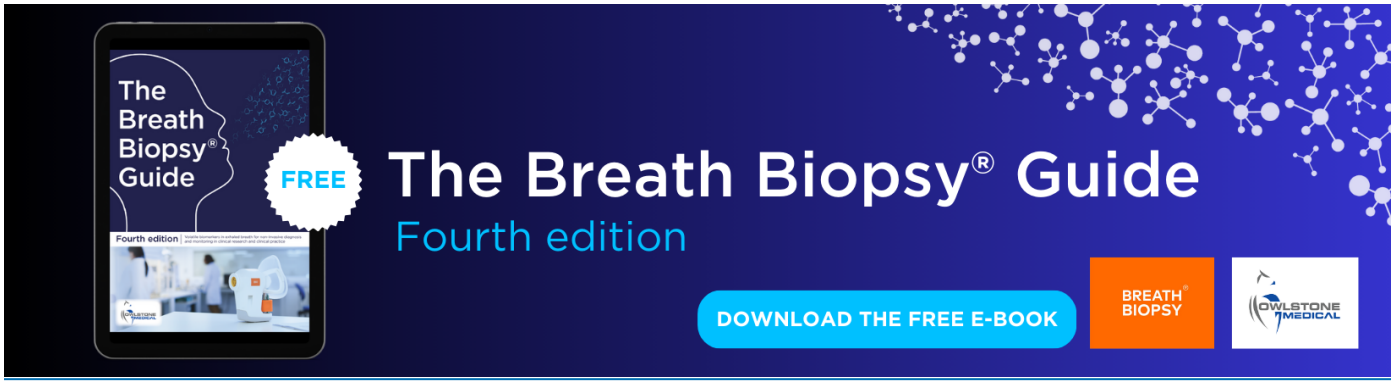

INSTITUTE OF PHYSICS PUBLISHING MEASUREMENT SCIENCE AND TECHNOLOGY

Meas. Sci. Technol. **17** (2006) 3293–3300 doi:10.1088/0957-0233/17/12/015

Magnetic field mapping around metal implants using an asymmetric spin-echo MRI sequence

K Bartusek[1,2], Z Dokoupil[1] and E Gescheidtova[2]

[1] Institute of Scientific Instruments, Academy of Sciences of the Czech Republic, Kralovopolska 147, 612 00 Brno, Czech Republic
[2] Faculty of Electrical Engineering and Communication, Brno University of Technology, Kolejni 2906/4, 612 00 Brno, Czech Republic

E-mail: bar@isibrno.cz and gescha@feec.vutbr.cz

Received 14 April 2006, in final form 13 October 2006
Published 7 November 2006
Online at stacks.iop.org/MST/17/3293

Abstract
Magnetic susceptibility of materials that are used for body implants causes much distortion in MR images. This paper deals with mapping the magnetic field induction in the vicinity of these materials. A modified spin-echo method is used, in which via inserting a time interval of a defined length the range of phase modulation is reduced below the value 2π. Even with a large B_0 inhomogeneity it is not necessary to unwrap the phase jumps. The method is suitable for studying the effects of body-implant materials on MR images and for measuring their magnetic susceptibility.

Keywords: nuclear magnetic resonance, spin echo, MRI, B_0 mapping, dental material

1. Introduction

An inhomogeneous static magnetic field (B_0 field) generates distortion in magnetic resonance (MR) images. Measuring the spatial variation of B_0 (B_0 field mapping) is essential for automatic shimming. It is also necessary for many image reconstruction methods that attempt to correct B_0 inhomogeneity-induced geometric distortions and signal losses. The dominant source of field inhomogeneity in many MRI experiments is the variation of magnetic susceptibility of both the tissues of the human body [1] and the implant materials [2].

Magnetic susceptibility provides information on the tissue relative iron concentration that is useful for diagnosis and treatment of a number of diseases such as sickle cell disease, aplastic anaemia, thalassemia, haemochromatosis and Parkinson's disease [3, 4]. In magnetic resonance imaging (MRI), the susceptibility effects have essential relevance for imaging contrast and artefact correction, functional brain imaging, molecular imaging and the measurement of blood oxygenation. Thus, it is highly significant to develop methods that can measure arbitrary susceptibility distributions. Many research efforts have been related to susceptibility quantification with non-invasive MR methods [5, 6]. A commonly used approach for susceptibility quantification in MRI is to measure the magnetic induction field deviations generated by magnetic susceptibilities on the basis of the frequency or phase of the MR signals [7, 8]. The same principle is used in the measurement of susceptibility by a gradient-echo MR method [9]. The susceptibility was determined from an MR phase image.

General biomedical applications often involve quantifying a susceptibility distribution in a localized region of interest (ROI). The field deviations in the ROI include three contributing components, i.e., the local susceptibility-induced magnetization, the magnet main field inhomogeneity, and the non-local demagnetizing fields generated by all the susceptibility distributions within the body and the susceptibility discontinuity at the body–air interface.

The distortion of MR images can be corrected using information provided by a field map [10–12]. With increasing use of high field imaging, the conventional field mapping method [12, 13], which calculates the phase differences between two gradient-echo images collected at different echo times (T_E), becomes unreliable because B_0 inhomogeneities at high field can cause signal dropouts and geometric distortions

in gradient-echo images. The phase map measured in a gradient-echo image depends on the evolution under the local magnetic field during T_E, but additional contributions to the accrued phase may arise due to the maximum signal not being centred in k-space, intrinsic T_2^* decay and imperfections in the excitation phase.

For the B_0 mapping of the magnetic field of humans the spin-echo sequence is used, with the gradient echo not aligned with the spin echo [21]. With this method, the changes in magnetic field called forth by the magnetic susceptibility of tissues are encoded in the phase of the MR image. The magnitude of phase change is proportional to the resonance frequency of the nuclei measured. This is utilized by Glover [22] to distinguish MR images of the brain weighted by water and fats. For this purpose he applies the three-point Dixon magnetic resonance imaging technique [23], which uses alternative water/fat phase-encoding strategies. The disadvantages of the method are the extra imaging time and the low S/N efficiency.

The spin-echo sequence (with the gradient echo not aligned with the spin echo) was used to characterize the deformations of B_0 magnetic field in the vicinity of measured specimens with a high magnetic susceptibility. The method is convenient for the mapping of B_0 magnetic field with inhomogeneity $\Delta B(x, y) < 2\pi/\gamma T_E$. With appropriately chosen magnitudes of an echo time $T_E \ll T_2$ and an additional time interval T_P the phase image modulation caused by inhomogeneity $\Delta B(x, y)$ will be less than 2π and it is thus not necessary to use the unwrapping [14] of phase images. The deformations of the basic magnetic field of an MR magnet show negatively in the B_0 maps measured, and the method described eliminates their effect.

2. MR measuring method

To map magnetic field induction by the magnetic resonance method the gradient-echo method is usually used [9, 24, 25]. The method is sensitive to the inhomogeneity of basic magnetic field, which distorts the MR image and is encoded in its phase. In the case of larger inhomogeneities of basic magnetic field it is necessary to unwrap the 2π phase jumps using the 2D unwrap function [20]. With a more complex spatial distribution of basic-field inhomogeneity ΔB_0 and with a higher level of noise in the image this procedure produces distortion and errors in the resultant image. To cope with this disadvantage, a modified spin-echo method was developed and experimentally tested, which via setting a time interval enables mapping of the B_0 inhomogeneity, similar to the gradient-echo method but, due to the large inhomogeneity $\Delta B(x, y)$, the phase coding will be within a range of 2π.

The spin-echo method, whose sequence in time is illustrated in figure 1, is a frequently used magnetic resonance imaging technique [9]. In the measuring sequence two RF excitation impulses are generated, whose duration is of the order of a few milliseconds. The first RF pulse, 90°, will excite the spin echo of the specimen being measured, and tilt the magnetization vector M_0, oriented in axis z, by 90° into a transversal (x, y) plane.

During the excitation pulse, a G_S gradient (slice-encoding gradient) is active, which is used to define the required layer z

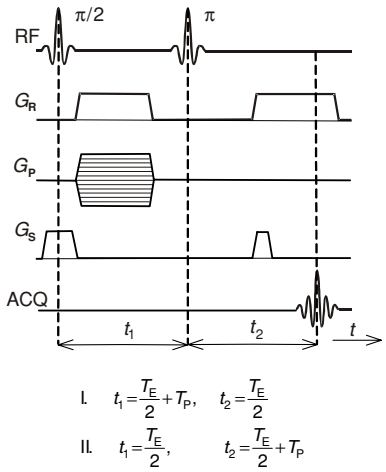

Figure 1. Measuring sequence SE with time interval T_P inserted into interval t_1 for mode I and into interval t_2 for mode II.

from the total volume of the specimen. With the G_R gradient (read-out gradient) acting in direction x (figure 1), the x coordinate of individual spins is coded into the frequency, which is in fact the frequency coding of the spin position. Simultaneously, a phase-encoding gradient G_P in direction y will encode the spins of the y coordinate into the phase of the MR signal, which is the phase encoding of the spin position. To encode the measured basic-field inhomogeneity $\Delta B_M(x, y)$ into the image phase and to produce spin-echo asymmetry a time interval T_P was inserted in the spin-echo sequence between excitation impulses of 90° and 180° (mode I) or between the excitation pulse and the acquisition start (mode II).

The total transversal magnetization from the excited layer (perpendicular to axis z representing the direction of the basic magnetic field) can be written as the equation

$$M_T(t) = \iint_{\text{slice}} m(x, y) \exp\left(\mathrm{j} \int \omega(x, y, t)\, \mathrm{d}t\right) \mathrm{d}x\, \mathrm{d}y, \qquad (1)$$

where $m(x, y)$ is the magnetization distribution of the measured layer.

For simplicity, the ideal situation is assumed in relation (1) and in the text below, which means that the magnetization is not affected by the relaxation time T_2. In a real case, the relaxation time T_2 affects the magnitude of the magnetization being measured, $m(x, y)$, and the signal-to-noise ratio of the image measured is the same as in the case of current SE techniques. Deviations from B_0 due to the presence of gradients and basic-field inhomogeneity $\Delta B_M(x, y)$ are considered. Thus the signal received is proportionate to the transversal magnetization.

On the assumption of zero duration of RF pulses in this model the evolution in time of transversal magnetization can be expressed by the substitution

$$\omega(x, y, t) = \gamma[\Delta B_M(x, y) + \mathbf{r} \cdot \mathbf{G}(t)], \qquad (2)$$

where γ is the gyromagnetic ratio, and $\mathbf{r}$ is the position vector.

The evolution in time of the exponent (phase) in (1) can be unwrapped for the gradients as depicted in figure 1 to yield

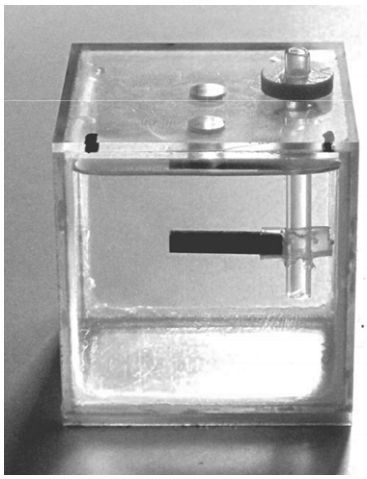

Figure 2. Specimen under measurement in a plastic holder.

$$\Phi(T_E + T_P) = \int_0^{T_E+T_P} \omega(x, y, t)\,dt$$
$$= -\gamma \left\{ \int_0^{T_E/2+T_P} \Delta B_M(x, y)\,dt + z \int_0^{T_E/2+T_P} G_z(t)\,dt + y \int_0^{T_E/2+T_P} G_{yn}(t)\,dt + x \int_0^{T_E/2+T_P} G_x(t)\,dt \right\}$$
$$+ \gamma \left\{ \int_{T_E/2+T_P}^{T_E+T_P} \Delta B_M(x, y)\,dt + z \int_{T_E/2+T_P}^{T_E+T_P} G_z(t)\,dt + x \int_{T_E/2+T_P}^{T_E+T_P} G_x(t)\,dt \right\}, \quad (3)$$

where the minus sign before the gyromagnetic ratio is due to the 180° pulse.

Each of the integrals describes the area under the gradient-versus-time curve (figure 1). It is seen from figure 1 and (3) that the terms with the z-gradient disappear (remember that the refocusing gradient lobe, associated with the slice selection pulse, has half the surface of the selection gradient). The term with the y-gradient remains, and the x-gradient waves are adjusted so that the area under the $G_x(t)$ curve is zero at $t = T_E + T_P$. This moment is chosen because it is the moment at which the spin-echo pulse refocuses the dephasing of static-field inhomogeneities. As a result of inserting the time interval T_P between pulses $\pi/2$ and π (mode I.), the phase at time $T_E + T_P$ will be

$$\Phi(T_E + T_P) = -\gamma \Delta B_M(x, y) T_P + \gamma G_{yn} T_y y, \quad (4a)$$

where T_y is the length of the gradient pulse G_{yn}.

As a result of inserting the time interval T_P between pulses π and acquisition (mode II), the phase at time $T_E + T_P$ will be

$$\Phi(T_E + T_P) = \gamma \Delta B_M(x, y) T_P + \gamma G_{yn} T_y y. \quad (4b)$$

The first term in (4*a*) expresses the spins being brought out of phase due to basic field inhomogeneities $\Delta B_M(x, y)$. The second term expresses the phase coding of the MR signal in axis y.

To establish the magnetization distribution in the layer being measured, it is necessary to integrate the time evolution of the angular frequency (2) during the MR signal acquisition time. After introducing the relative time with respect to time $T_E + T_P$, i.e. $t' = t - T_E - T_P$, equation (3) can be rewritten in the form

$$\int_0^t \omega(x, y, t)\,dt = -\Delta B_M(x, y) t' + \gamma G_{yn} T_y y + \gamma G_x t' x$$
$$= k_y y + k_x \left(x - \frac{\Delta B_M(x, y)}{G_x} \right), \quad (5)$$

where k_y and k_x are the integration constants dependent on time

$$k_x = \gamma G_x t' = \gamma \int_0^{t'} G_x(t)\,dt$$

and

$$k_y = \gamma G_{yn} T_y = \gamma \int_0^{t'} G_{yn}(t)\,dt. \quad (6)$$

The expression for the total magnetization (1) in a layer parallel to the (x, y) plane can be rewritten in the form

$$M_T(t') = \iint_{xy} m(x, y) \times \exp\left(-j \left(k_x \left(x - \frac{\Delta B_M(x, y)}{G_x} + k_y Y \right) \right) \right) \times \exp(-j\gamma \Delta B_M(x, y) T_P)\,dx\,dy. \quad (7)$$

Equation (7) is the fundamental relation for MR imaging (2D acquisition) and it is the expression of a function in time using a double integral that is in the form of a two-dimensional Fourier transform. At any instant of time t we know the values

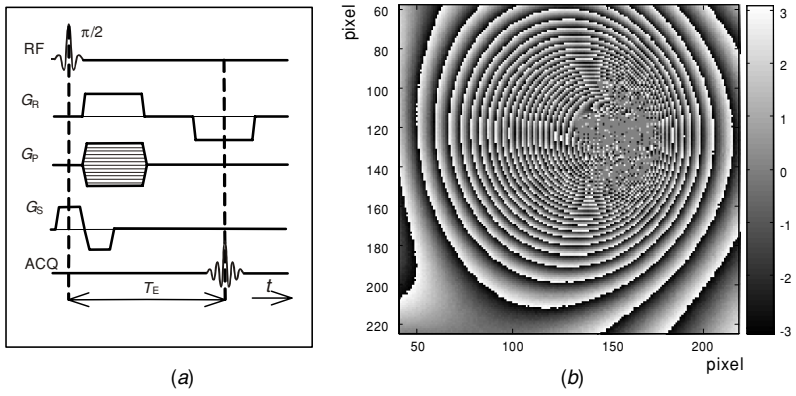

Figure 3. Phase image of a Co–Cr–Mo alloy cylinder, scanned by the gradient-echo method with echo time $T_E = 5.66$ ms.

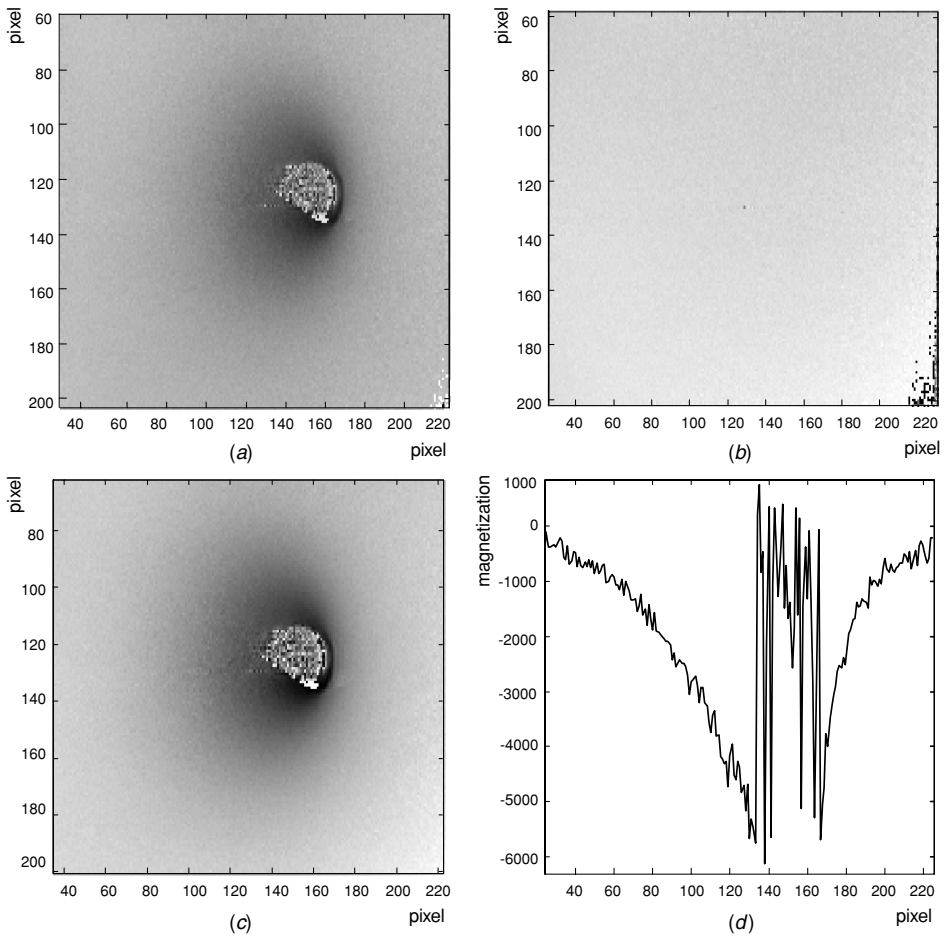

Figure 4. Phase image of a cylinder of Co–Cr–Mo alloy scanned by the spin-echo method, with interval $T_P = 0.15$ ms.

of $k_x(t)$ and $k_y(t)$ (6) so that we can write $M_T(t')$ as $M_T(k_x, k_y)$. Equation (7) thus defines the so-called Fourier pair $m(x, y)$ and $M_T(k_x, k_y)$ and is in fact a mapping of function $m(x, y)$ in the (x, y) plane onto function $M_T(k_x, k_y)$ in the (k_x, k_y) plane. The expression $\Delta B_M(x, y)/G_x$ in (5) and (7) causes a deformation of the $m'(x, y)$ image. This issue is explained in [26]. The inverse transform of $M_T(k_x, k_y)$ gives not $m'(x, y)$, but a distorted version of it, distorted by a geometrical shift and change of image intensity. It can be seen from (7) that the reconstructed image $m'(x, y)$ (via the Fourier transform with the assumption of negligible $\Delta B_M(x, y)/G_x$) will be

$$m'(x, y) = m(x, y) \exp(-\gamma \Delta B_M(x, y) T_P). \tag{8}$$

In relation (8) the exponential $\exp(-j\gamma \Delta B_M(x, y) T_P)$ expresses encoding the inhomogeneity of the basic field into the image phase. A change in the image phase by 2π corresponds to the change in the magnetic induction

$$\Delta B_M(x, y) = -\frac{1}{\gamma' T_P}, \tag{9}$$

where $\gamma' = \gamma/2\pi$.

After rewriting for an arbitrary phase change $\Delta\Phi$ the magnetic induction will be

$$\Delta B_M(x, y) = -\frac{\Delta\Phi}{\gamma' T_P}. \tag{10}$$

If the condition $\Delta\Phi < 2\pi$ is satisfied, it is not necessary to unwrap the phase of the image being measured. The maximum length of time interval T_P can be determined according to the relation

$$T_P \leqslant \frac{2\pi}{\gamma' \Delta B_M(x, y)}. \tag{11}$$

In the case of unknown inhomogeneity $\Delta B_0(x, y)$ the time interval T_P is set to zero and, based on the magnitude of $\Delta B_0(x, y)$ estimated from the number of 2π phase jumps in the phase image, the calculation of T_P according to relation (11) is performed.

In relations (8) and (9) the term $\left(x - \frac{\Delta B_M(x,y)}{G_x}\right)$ expresses the distortion in the MR image due to the basic field inhomogeneity $\Delta B_M(x, y)$. With large magnetic field deformation in comparison with the magnitude of the gradient used there is a shift in the image in the read-out direction. To reduce this effect it is possible to use a larger gradient amplitude or a mathematical transformation in the image being measured.

In the present paper the maximum $\Delta B_M(x, y)/G_x$ ratio was 0.0125 and thus the effect of the shift term was neglected. The measured map of magnetic field $\Delta B_M(x, y)$ includes the magnetic field inhomogeneity caused by the susceptibility of measured specimen $\Delta B(x, y)$, by the inhomogeneity of the magnetic field of the background $\Delta B_0(x, y)$, by the created

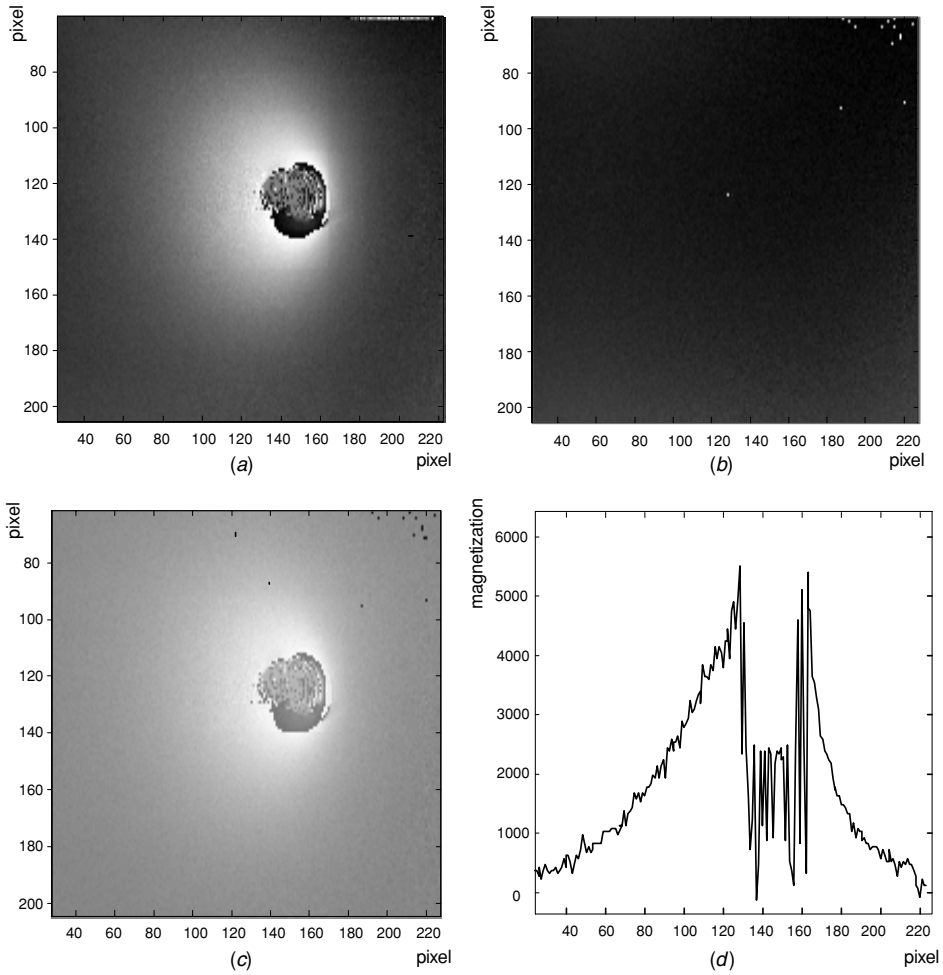

Figure 5. Phase image of a cylinder of Co–Cr–Mo alloy scanned by the spin-echo method, with interval $T_P = 0.15$ ms inserted between the $\pi/2$ pulse and the π RF pulse.

inhomogeneity of the basic magnetic field of the working space of the MR magnet, and by the field inhomogeneity caused, for example, by the susceptibility of the holder of material. To establish an accurate map of magnetic field $\Delta B(x, y)$ it is always necessary to subtract from the measured map of field $\Delta B_M(x, y)$ the map of background field $\Delta B_0(x, y)$, which is measured under identical conditions (but without the specimen measured) according to the relation

$$\Delta B(x, y) = \Delta B_M(x, y) - \Delta B_0(x, y). \tag{12}$$

3. Experimental results

The above method was tested experimentally on a 4.7 T/120 mm MR scanner with an actively shielded gradient system when studying the effect of materials for dental implants on the distortion of the MR mapping. The distortion of basic magnetic field B_0 was mapped in the vicinity of cylindrical specimens (20 mm in length, 4 mm in diameter) of two dental materials of different susceptibilities, which had been placed in a plastic holder and immersed in water, figure 2. One specimen was a Co–Cr–Mo alloy (Co, Cr, Mo,C, Fe, Mn, Si) with a high value of magnetic susceptibility ($\chi = 1370 \times 10^{-6}$) and conductivity ($\rho = 1.26$ S m mm^{-2}). The other material was an amalgam of Ag–Sn–Cu composition (Ag, Sn, Cu, Hg), which has a higher conductivity $\rho = 3.41$ S m mm^{-2} and magnetic susceptibility $\chi = -25 \times 10^{-6}$.

For the sake of quantitative comparison the phase MR image was measured by the usual gradient-echo method [22], figure 3(*a*), for the Co–Cr–Mo alloy. In laboratory coordinates the image is 60×60 mm^2 and contains 256×256 pixels. With a slice selection gradient of 63.5 mT m^{-1} (2700 Hz mm^{-1}), a layer 1 mm thick was defined, oriented perpendicular to B_0. In view of the specimen symmetry, the distortion of the selected layer (<1 mm) can be neglected. The 2π phase jump for the echo time $T_E = 5.66$ ms corresponds to the change in magnetic field $\gamma' \Delta B_{2\pi} = 177$ Hz. It is obvious from figure 3(*b*) that in its vicinity the material being measured will cause a change in magnetic field induction >94 μT (>4000 Hz).

In the case of specimens with a larger susceptibility there is a large spatial gradient of magnetic field close to the specimen surface. For the Co–Cr–Mo alloy with susceptibility $\chi = 1370 \times 10^{-6}$ the maximum change in magnetic field in one image pixel is $\gamma' \Delta B_p = 175$ Hz/pixel (figures 3 and 4). This inhomogeneity reduces the MR signal from one image pixel to 5.7 ms. Since the signal is detected at time $T_E = 5.56$ ms, the amplitude of MR image in the close vicinity

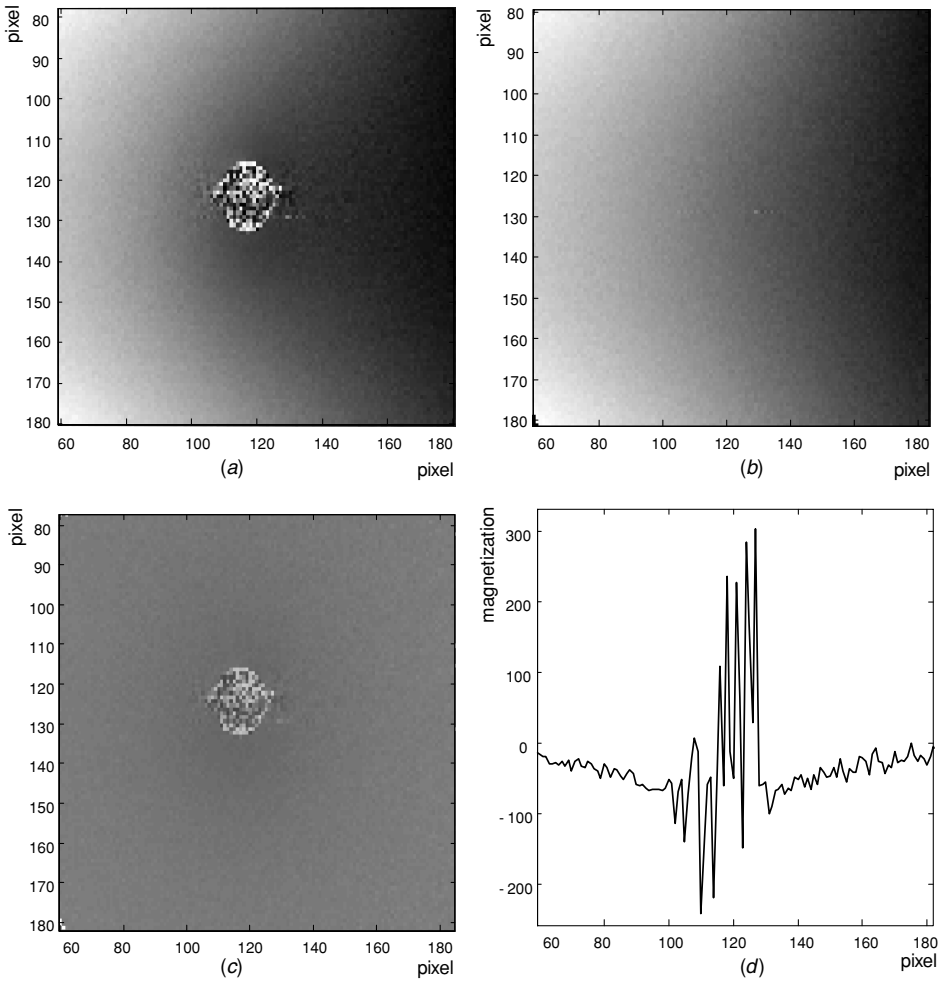

Figure 6. Phase image of a cylinder of Ag–Sn–Cu alloy scanned by the spin-echo method, with interval $T_P = 0.15$ ms inserted between the $\pi/2$ pulse and the π pulse.

of the specimen being measured will drop to 0.38 and the signal-to-noise ratio in the image will also be reduced. A large spatial gradient can even lead to the MR signal being lost near the specimen.

For a change in the magnetic field in the vicinity of a dental material specimen (Co–Cr–Mo alloy) exceeding 4000 Hz the chosen length of time interval in the spin-echo sequence was $T_P = 0.15$ ms, which corresponds to $\gamma' \Delta B_{2\pi} = 6667$ Hz. Figure 4(*a*) illustrates the phase image of 1 mm slice perpendicular to B_0 for inserting the time interval T_P between impulses $\pi/2$ and π (mode I), and without any further processing by the unwrap function. Figure 4(*c*) shows the image of the magnetic field inhomogeneity in the vicinity of the specimen under measurement, after subtracting the B_0 inhomogeneity background (without the specimen), which is shown in figure 4(*b*). Figure 4(*d*) shows the waveform of magnetic field passing in the read-out direction through the centre of the specimen being measured.

The resultant maps of field $\Delta B(x, y)$ when a time interval $T_P = 0.15$ ms is inserted between the π impulse and the start of acquisition (mode II) are given in figure 5. Figure 5(*a*) is the phase image of an 1 mm slice perpendicular to the specimen. After subtracting the map of $\Delta B_0(x, y)$ inhomogeneity, figure 5(*b*), we obtain the image of the $\Delta B(x, y)$ map in the specimen surround, figure 5(*c*). The waveform of magnetic field in the slice going through the specimen centre in the read-out direction is given in figure 5(*d*).

The method described above was used to measure the map of $\Delta B(x, y)$ magnetic field in the vicinity of a specimen of low susceptibility (Ag–Sn–Cu amalgam) for mode I. The resultant map and slice through the specimen centre are given in figures 6(*a*)–(*d*).

4. Discussion

In the mapping of $\Delta B(x, y)$ field by the gradient-echo method it is impossible to obtain a spin-echo time T_E shorter than several milliseconds (<3 ms), and the phase change $\Delta\Phi = 2\pi$ is obtained for $\gamma \Delta B_{(2\pi)} < 300$ Hz. This change is due to the low susceptibility of the tissue.

Using the method of asymmetric spin echo and with the time interval in the range $0.1 < T_P < 5$ ms it is possible to increase $\gamma \Delta B_{(2\pi)}$ to as much as 10 000 Hz. A reduction in T_P necessarily increases the effect of inaccuracies in the measuring sequence such as the decay of magnetic field gradients, time sampling of gradients, setting the $\pi/2$ and

π excitation pulses, accuracy of time intervals, etc. These effects reduce the measuring accuracy in the case of high tissue susceptibilities and can thus constrain some measurements.

In the spin-echo sequence the time T_E is always longer than in the gradient-echo sequence and therefore the SNR in the image measured is always lower than with the gradient-echo method. In the case of high susceptibilities that entail large inhomogeneity of the magnetic field there are losses in the MR signal, which are not negligible and are due to the MR signal being brought out of phase to the extent of one image pixel. With the spin-echo method, the loss in the MR signal will be smaller due to the small time interval T_P. Time T_E of the spin-echo sequence can be made shorter by shortening the time between pulse π and acquisition. This will enable measuring specimens with shorter relaxation times T_2.

The time interval T_P was inserted into the spin-echo sequence between two excitation impulses without the presence of gradients. In this case by relations (3) and (10) the phase modulation has a negative sign. Inserting the time interval T_P between the π impulse and the acquisition start will not change the resultant map of field $\Delta B(x, y)$ but the phase modulation will be of opposite sign. For the mapping of field B_0 both possibilities of placing the time interval T_P can be used with advantage.

The distortion in the image due to the inhomogeneity of basic field $\Delta B(x, y)$ is the same irrespective of whether the gradient-echo or the spin-echo method is used. Its size depends on the ratio of the maximum inhomogeneity of the basic field to the magnitude of the gradient G_x. To constrain this artefact, a higher gradient amplitude or a mathematical transformation can be used in the image being measured.

To verify the result expected, a simulation of centrally symmetrical lay-out was carried out by the FEM in the ANSYS program, under the same conditions as in the real measurement [2, 9, 22]. The calculation started from the Laplace equation, and the spatial lay-out of stationary magnetic field in the neighbourhood of the specimen being measured was calculated. The calculation results agree with the experiment.

5. Conclusion

The above-described MR method of measuring was used for the study of distortions in MR images caused by the properties of the measured tissues and by the materials of dental and body implants. So far, the results of the above studies have not been published comprehensively but it is already obvious that they will affect the choice of materials used in dentistry. The method described above has made it possible to do away with problems with 2D unwrapping of phase images, and with the ambiguity of unwrapping. The accuracy has been increased of determining the magnitude of magnetic susceptibility of specimens being measured, and the effect of the magnetic background of the specimen has been eliminated. In contrast to other mapping methods, it is sufficient to measure one phase image.

The method is suitable for the measurement of magnetic properties of materials and tissues of high magnetic susceptibility.

Acknowledgments

This work has been supported by the Grant Agency of the Ministry of Health of the Czech Republic (IGA MZCR 8110-3/2004) and with the support of the research plans MSM 0021630516.

References

[1] Jezzard P and Clare S 1999 Sources of distortion in functional MRI data *Hum. Brain Mapp.* **8** 80–5
[2] Starcuk Z, Hubalkova Z, Krupa P, Bartusek K, Starcukova J and Linetskiy I 2005 Assessment of MR compatibility of selected dental alloys *Proc. 13th Scientific Meeting of Int. Soc. for Magnetic Resonance in Medicine (Miami Beach, FL, USA)* p 2276
[3] Brittenham G and Badman D Noninvasive measurement of iron *Report of an NIDDK Workshop. Blood 2002* pp 15–9
[4] Bartzokis G, Cummings J L, Markham C H, Marmarelis P Z, Treciokas L J, Tishler T A, Marder S R and Mintz J 1999 MRI evaluation of brain iron in earlier and later-onset Parkinson's disease and normal subjects *Magn. Reson. Imaging* **17** 213–22
[5] Schenck J F 1996 The role of magnetic susceptibility in magnetic resonance imaging: MRI magnetic compatibility of the first and second kinds *Med. Phys.* **23** 815–50
[6] Ro Y M and Cho Z H 1995 Susceptibility magnetic resonance imaging using spectral decomposition *Magn. Reson. Med.* **33** 521–8
[7] Chu S C, Xu Y, Balschi J A and Springer C S Jr 1990 Bulk magnetic susceptibility shifts in NMR studies of compartmentalized samples: use of paramagnetic reagents *Magn. Reson. Med.* **13** 239–62
[8] Wang Z J, Li S and Haselgrove J C 1999 Magnetic resonance imaging measurement of volume magnetic susceptibility using a boundary condition *J Magn. Reson.* **140** 477–81
[9] Steinbauer M and Bartusek K 2005 Magnetic properties of materials—comparison of NMR and inductive measuring methods *28th Int. Conf. on Fundamentals of Electrotechnics and Circuit Theory SPETO (Gliwice, Poland)* pp 67–70
[10] Marques J P and Bowtell R 2005 Application of a Fourier-based method for rapid calculation of field inhomogeneity due to spatial variation of magnetic susceptibility *Concepts Magn. Reson.* B **25** 65–78
[11] Jenkinson M, Wilson J and Jezzard M 2003 Modelling B_0 induced artefacts in fMRI using perturbation calculations *Aust. J. Psychol.* **55** 21 (Suppl)
Hutton S *et al* 2002 Image distortion correction in fMRI: a quantitative evaluation *Neuroimage* **16** 217–40
[12] Schneider E and Glover G 1991 Rapid *in vivo* proton shimming *Magn. Reson. Med.* **18** 335
[13] Li L and Leigh J S 2004 Quantifying arbitrary magnetic susceptibility distributions with MR *Magn. Reson. Med.* **51** 1077–82
[14] Ghiglia D C and Pritt M D 1998 *Two-Dimensional Phase Unwrapping* (New York: Wiley)
[15] Hopkins J A and Wehrli F W 1997 Magnetic susceptibility measurement of insoluble solids by NMR: magnetic susceptibility of bone *Magn. Reson. Med.* **37** 494–500
[16] Weisskoff R M and Kiihne S 1992 MRI susceptometry: image-based measurement of absolute susceptibility of MR contrast agents and human blood *Magn. Reson. Med.* **24** 375–83
[17] Holt R W, Diaz P J, Duerk J L and Bellon E M 1994 MR susceptometry: an external phantom method for measuring bulk susceptibility from field-echo phase reconstruction maps *J. Magn. Reson. Imaging* **4** 809–18
[18] Young I R, Khenia S, Thomas D G, Davis C H, Gadian D G, Cox I J, Ross B D and Bydder G M 1987 Clinical magnetic

susceptibility mapping of the brain *J. Comput. Assist. Tomogr.* **11** 2–6
[19] Zhao Y, Zeng H and Gore J C 2005 B_0 field mapping with a fast asymmetric spin echo sequence at high field *Magn. Reson. Med.* **13** 2248
[20] Beuf O, Briguet A, Lissac M and Davis R 1996 Magnetic resonance imaging for the determination of magnetic susceptibility of materials *J. Magn. Reson.* B **112** 111–8
[21] Munger P 1994 Accuracy considerations in MR image-guided neurosurgery *Thesis* Department of Physics, McGill University, Montreal
[22] Dixon W T 1984 Simple proton spectroscopic imaging *Radiology* **153** 189
[23] Glover G H 1991 Multipoint Dixon technique for water and fat proton and susceptibility imaging *J. Magn. Reson. Imaging* **1** 521–30
[24] Haacke E M, Brown R W, Thompson M R and Venkatesan R 1999 *Magnetic Resonance Imaging—Physical Principles and Sequence Design* (New York: Wiley-Liss)
[25] Steinbauer M 2005 Magnetic susceptibility measurement by means of MRI technique. *Doctoral Thesis* BUT Brno, Czech Republic (in Czech)
[26] Park H W, Ro Y M and Cho Z H 1988 Measurement of the magnetic susceptibility effect in high-field NMR imaging *Phys. Med. Biol.* **33** 339–49